Aeolian Sediment Supply at a Mega Nourishment

Bas Hoonhout[a,b,*], Sierd de Vries[a]

[a] *Delft University of Technology, Faculty of Civil Engineering and Geosciences, Department of Hydraulic Engineering, Stevinweg 1, 2628CN Delft, The Netherlands.*
[b] *Deltares, Department of Hydraulic Engineering, Boussinesqweg 1, 2629HV Delft, The Netherlands.*

Abstract

Mega nourishments are intended to enhance growth and resilience of coastal dunes on medium to long time scales by stimulation of natural sediment transport processes. The growth and resilience of coastal dunes largely depends on the presence of a continuous supply of aeolian sediment. A recent example of a mega nourishment is the 21 Mm^3 mega nourishment known as the Sand Motor. The Sand Motor is intended to nourish the entire Holland coast over a period of two decades. Four years of bi-monthly topographic measurements of the Sand Motor domain provide an opportunity to analyze spatiotemporal variations in aeolian sediment supply using an aeolian sediment budget analysis. It appears that more than 58% of all aeolian sediment deposits originate from the low-lying beaches that are regularly reworked by waves. Aeolian sediment supply from higher beaches diminished after half a year after construction of the Sand Motor, likely due to the formation of deflation lag deposits that constitute a beach armor layer. The compartmentalization of the Sand Motor in armored and unarmored surfaces suggests that the construction height is an important design criterion that influences the lifetime and region of influence for any mega nourishment.

Keywords: aeolian sediment transport; aeolian sediment supply; beach armoring; sediment budgets; mega nourishment; Sand Motor

1. Introduction

Aeolian sediment supply is a prerequisite to growth and resilience of coastal dunes that function as a natural protection against flooding from the sea. Expanding human activities in coastal areas and growing uncertainties related to climate change, increase coastal risks. Mitigation of these risks

Email addresses: b.m.hoonhout@tudelft.nl (Bas Hoonhout), bas.hoonhout@deltares.nl (Bas Hoonhout)

resulted in the engineering of entire coastlines (Donchyts et al., 2016). Rigid solutions and local nourishments are traditional solutions to a societal demand for coastal safety (Hamm et al., 2002). With the increased confidence in our ability to mitigate coastal risks, additional demands and functions for coastal flood protections arose. Soft engineering solutions with limited environmental and ecological impact (Waterman, 2010; de Vriend et al., 2015) gained preference over rigid solutions or local nourishments. Recently, the exponent of soft engineering emerged as mega nourishments (Stive et al., 2013). Mega nourishments pursue the idea of stimulating natural sediment transport processes with the aim of increasing coastal safety. The idea is based on the assumption that the incidental or concentrated interventions necessary for the stimulation of nature are less intrusive than classic solutions to coastal safety. Moreover, mega nourishments tend to accommodate long-term monitoring and periodic adaptation and intervention that increases flexibility with respect to planning and execution as well as the occurrence of coastal hazards. The increased flexibility can make mega nourishments also cost-effective (Van Slobbe et al., 2013).

The effectiveness of a mega nourishment depends on the sediment transport pathways from nourishment to dunes. A small fraction of the sediment moved in the nearshore ultimately arrives in the dunes (Aagaard et al., 2004). It is this small aeolian sediment supply that provides us with the natural and persistent coastal safety that mega nourishments aim for. In addition, this small aeolian sediment supply gives coastal dune systems the natural resilience to storm impacts and the conditions for survival of persistent dune vegetation that strengthens the dunes, like marram grass (Borsje et al., 2011). It is also this small aeolian sediment supply that is least understood.

Mega nourishments affect aeolian sediment supply to coastal dunes in various ways. First, sand used for nourishment is typically obtained from offshore borrowing pits and differs from the original beach sand in terms of size and composition, affecting the erodibility of the beach (van der Wal, 1998, 2000). Second, aeolian sediment availability (following the definition of Kocurek and Lancaster, 1999) at beach nourishments that are constructed above storm surge level can be significantly reduced by deflation lag deposits (Jackson et al., 2010). The absence of regular flooding and wave-reworking allows lag deposits to develop a beach armor layer, resulting in compartmentalization of the nourishment in armored and unarmored surfaces. McKenna Neuman et al. (2012) illustrated how deflation lag deposits increase the shear velocity threshold significantly and reduce aeolian sedi-

ment availability and subsequently supply from the higher supratidal beach. Deflation lag deposits can therefore cause intertidal and low-lying supratidal beaches to gain importance over the high and dry beach as source of aeolian sediment. Third, the placement of a nourishment is known to affect nearshore processes (Grunnet and Ruessink, 2005; Ojeda et al., 2008; De Schipper et al., 2013). Synchronization between aeolian and nearshore processes, like onshore bar migration and welding, is reported to stimulate aeolian sediment supply to coastal dunes (Houser, 2009; Anthony, 2013). The importance of low-lying beaches as source of aeolian sediment might therefore also be affected by changing bar dynamics.

Jackson and Nordstrom (2011) emphasized the necessity for the quantification of the effect of large scale beach nourishment designs on aeolian sediment supply. Quantitative predictions of aeolian sediment availability and supply in coastal environments has proven to be challenging (Sherman et al., 1998; Sherman and Li, 2012). Limitations in aeolian sediment availability are often identified as reason for the discrepancy between measured and predicted sediment transport rates (Delgado-Fernandez et al., 2012; de Vries et al., 2014; Lynch et al., 2016).

Mega nourishments inherently cause spatiotemporal variations in aeolian sediment availability. The spatial variations are caused by compartmentalization of the beach. The temporal variations are induced by adaptation of the large coastal disturbance to the wave and wind climate, resulting in changing in beach width, slope and composition (de Schipper et al., 2016). Consequently, quantification of aeolian sediment availability and supply from mega nourishments requires differentiation in space and time.

This paper presents an aeolian sediment budget analysis of the 21 Mm^3 Sand Motor mega nourishment based on four years of bi-monthly topographic surveys. The sediment budget analysis quantifies the net aeolian sediment supply to the dunes, dune lake and lagoon accommodated by the Sand Motor. The Sand Motor constitutes distinct areas that are either influenced by marine processes, by aeolian processes or by a combination of both. Therefore, the influence of marine and aeolian processes on aeolian sediment supply can be separated and spatiotemporal variations in aeolian sediment availability can be identified with reasonable accuracy. The observed compartmentalization of the Sand Motor is discussed in relation to limitations in aeolian sediment availability, as well as the design of mega nourishments like the Sand Motor as solution to coastal safety.

2. Field Site

The Sand Motor (or Sand Engine) is an artificial 21 Mm^3 sandy peninsula protruding into the North Sea off the Delfland coast in The Netherlands (Figure 1, Stive et al., 2013). The Sand Motor is an example of a mega nourishment and is intended to nourish the Holland coast for a period of two decades, while stimulating both biodiversity and recreation.

The Sand Motor was constructed in 2011 and its bulged shoreline initially extended about 1 km seaward and stretched over approximately 2 km along the original coastline. The original coast was characterized by an alongshore uniform profile with a vegetated dune with an average height of 13 m and a linear beach with a 1:40 slope. The dune foot is located at a height of approximately 5 m+MSL.

Due to natural sediment dynamics the Sand Motor distributes about 1 Mm^3 of sand per year to the adjacent coasts (Figure 1). The majority of this sand volume is transported by tides and waves. However, the Sand Motor is constructed up to 5 m+MSL and locally up to 7 m+MSL, which is in either case well above the maximum surge level of 3 m+MSL (Figure 2c). Therefore, the majority of the Sand Motor area is uniquely shaped by wind.

The Sand Motor comprises both a dune lake and a lagoon that act as large traps for aeolian sediment (Figure 1). The lagoon is affected by tidal forcing, although the tidal amplitude quickly diminished over time as the entry channel elongated. The tidal range of about 2 m that is present at the Sand Motor periphery (Figure 2c), is nowadays damped to less than 20 cm inside the lagoon (de Vries et al., 2015). Consequently, the tidal currents at the closed end of the lagoon, where most aeolian sediment is trapped, are negligible.

Sand used for construction of the Sand Motor is obtained from an offshore borrowing pit in the North Sea. The sand is predominantly Holocene sand with a significant amount of fines. The median grain size is slightly coarser than found originally along the Delfland coast. Apart from sand fractions, the sediment contains a large amount of shells, shell fractions, some pebbles and cobbles and an occasional fraction of a mammoth bone.

The dominant wind direction at the Sand Motor is south to southwest (Figure 2a). However, during storm conditions the wind direction tends to be southwest to northwest. During extreme storm conditions the wind direction tends to be northwest. Northwesterly storms are typically accompanied by significant surges as the fetch is virtually unbounded to the northwest, while

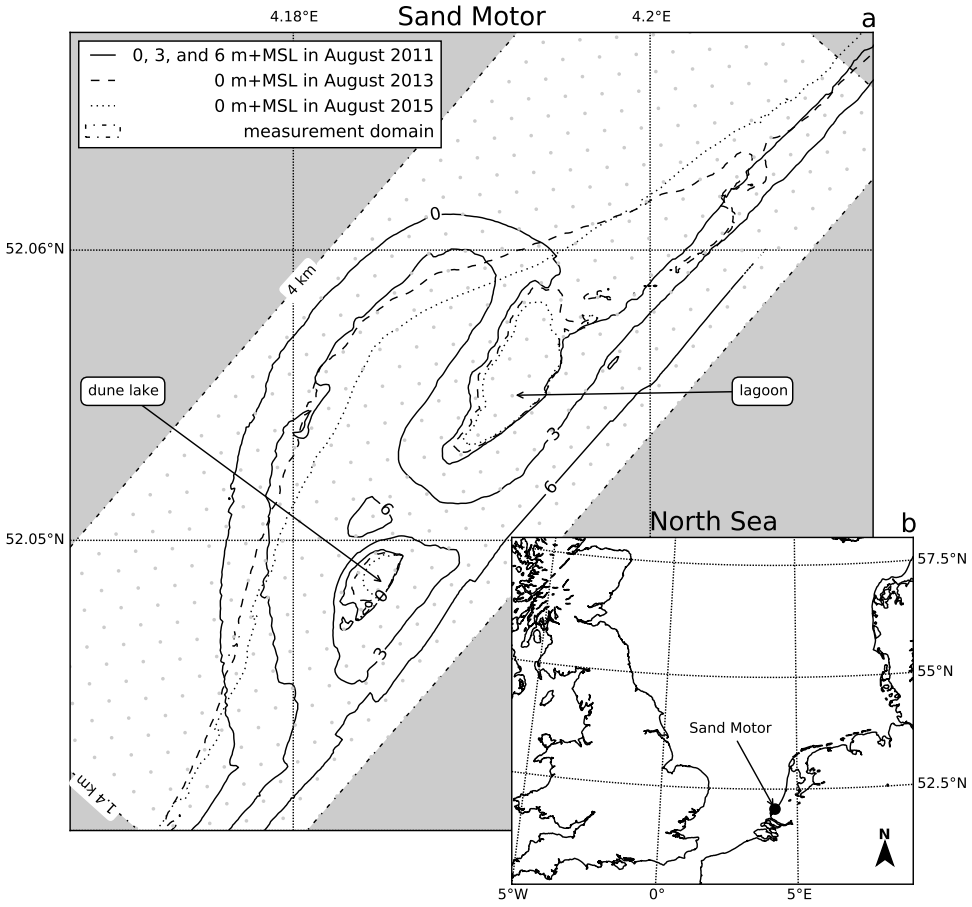

Figure 1: Location, orientation, appearance and evolution of the Sand Motor between construction in 2011 and 2015. The box indicates the measurement domain used in the remainder of this paper. A 100 x 100 m grid aligned with the measurement domain is plotted in gray as reference.

surges from the southwest are limited due to the presence of the narrowing of the North Sea at the Strait of Dover (Figure 1, inset).

3. Methodology

Spatiotemporal variations in aeolian sediment supply in the Sand Motor domain are identified using an aeolian sediment budget analysis. A sediment budget analysis can be performed if frequent topographic measurements are available (Davidson-Arnott and Law, 1990) and sediment exchange over the border of the measurement domain is limited. In a sediment budget analysis the morphological change in predetermined areas are converted to volumetric changes (budgets) that are compared in a sediment volume balance.

A sediment budget analysis is particularly suitable for coastal sites with a complex and dynamic topography, like the Sand Motor. The use of (dense) topographic measurements ensures that any local variations in the topography are included. Moreover, no assumptions on the local representativeness of the measurements are needed. The methodology is applicable to a wide range of spatial or temporal scales, allowing a multi-annual analysis of aeolian sediment supply in the Sand Motor domain.

In the Sand Motor domain it is possible to separate the marine and aeolian influence on erosion and deposition of sediment directly from a sediment budget analysis. The high construction height of the Sand Motor and the absence of regular storm surges in the first four years after construction make that distinct areas exist that are either influenced by marine or aeolian processes. The sediment budgets are determined along the borders of these marine and aeolian zones.

3.1. Topographic measurements

32 topographic measurements of the Sand Motor domain obtained over a period of four years are used to determine the overall sediment budget of the Sand Motor domain (de Schipper et al., 2016). The measurement area covers 1.4 km cross-shore and 4 km alongshore (Figure 1). The nearshore bathymetry is surveyed using a jetski equipped with an echo sounder and RTK-GPS receiver. The topography of the Sand Motor from the waterline up to the dune foot is surveyed using an all-terrain vehicle (ATV) that is also equipped with a RTK-GPS receiver. Inundated areas that are too shallow for the jetski, like the tidal channel and the dune lake, are surveyed using a manually pushed RTK-GPS wheel. The survey is performed along

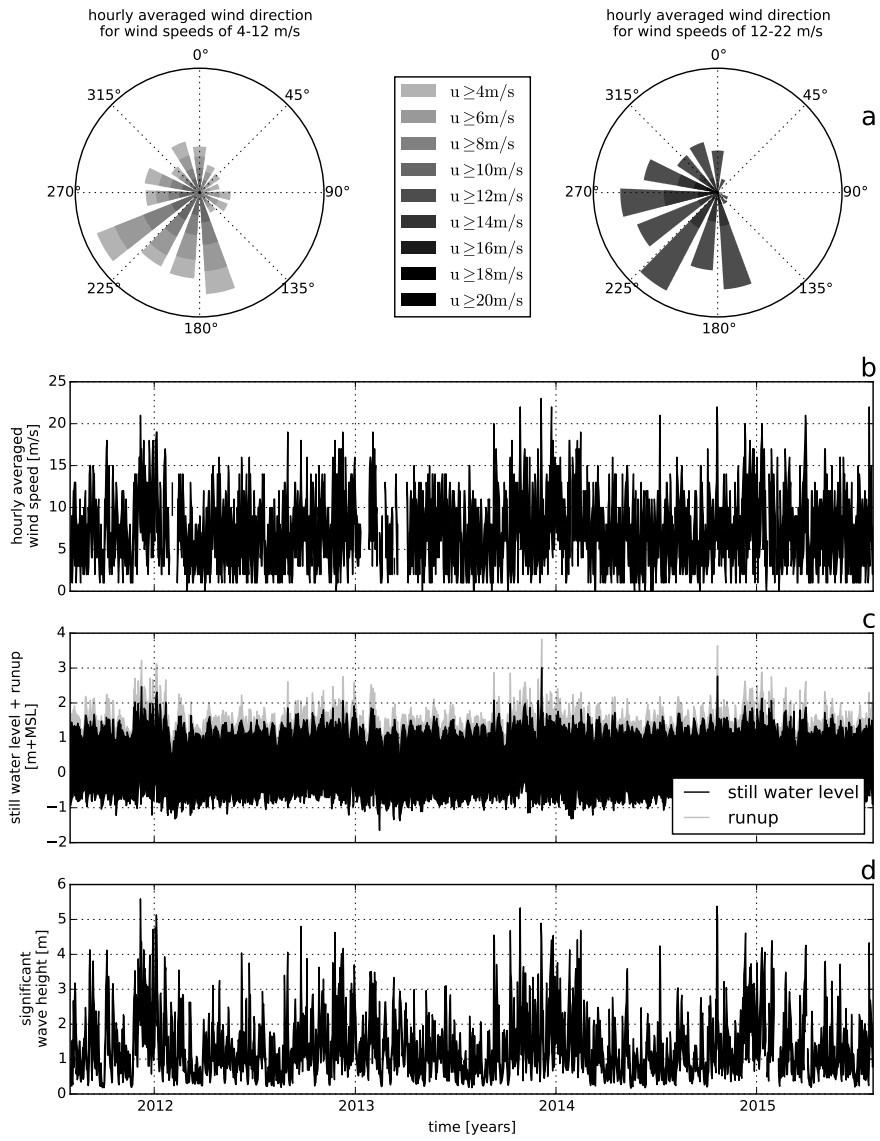

Figure 2: Wind and hydrodynamic time series from 2011 to 2015. Hourly averaged wind speeds and directions are obtained from the KNMI meteorological station in Hoek van Holland (upper panels). Offshore still water levels, wave heights and wave periods are obtained from the Europlatform (lower panels). Runup levels are estimated following Stockdon et al. (2006).

cross-shore transects that are 20 m apart. The resulting trajectories are interpolated to a regular 10 m x 10 m grid for the sediment budget analysis. Surveys that show a morphological rate of change that is more than two standard deviations from the average are considered outliers. The measurements of September 4, 2011 and June 21, 2012 are discarded as outliers.

The topography in the dune area, which is not included in the RTK-GPS surveys, is monitored by airborne lidar. Half-yearly measurements from the southern Holland coast (Delfland coast) are available since 2011, prior to the construction of the Sand Motor. The lidar measurements have a spatial resolution of 2 m or 5 m. The measurements are corrected for the presence of vegetation and artificial objects, like beach pavilions, and interpolated to the same 10 m x 10 m grid and the same moments in time as the RTK-GPS measurements.

3.2. Zonation

The Sand Motor domain is divided into seven zones for the aeolian sediment budget analysis (Table 1 and Figure 3). The zonation aims to separate areas with marine influences from areas without marine influences, and separate areas with net aeolian erosion from areas with net aeolian deposition.

Table 1: Zonation of the Sand Motor domain into seven zones with and without marine influence. See also Figure 3.

without marine influence	*with* marine influence
aeolian zone	mixed zone (north)
dunes	mixed zone (south)
dune lake	marine zone
lagoon	

The zonation is based on the 0 m+MSL, 3 m+MSL and 5 m+MSL contour lines that roughly correspond to mean sea level, the edge of the berm or maximum runup level (Figure 2c) and the dune foot respectively. The contours are determined such that the spatial variance in the bed level change of the zones is minimized. The minimization ensures that the optimal division between erosion and deposition areas is found. Moreover, the 3 m+MSL and 5 m+MSL contour lines have been relatively static since construction of the Sand Motor.

To ensure a constant shape and size of the zones during the analysis, the convex hull of all 3 m+MSL contour lines is used as zone boundary for

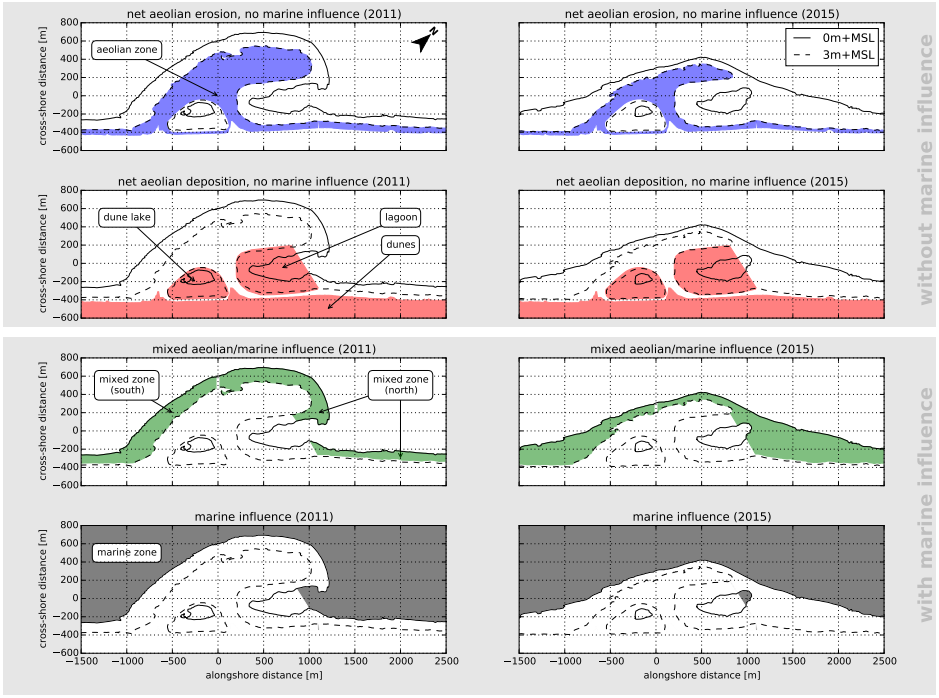

Figure 3: Zonation of the Sand Motor domain into zones with net aeolian erosion and no marine influence, net aeolian deposition and no marine influence, mixed aeolian/marine influence and marine influence. Left panels: 2011. Right panels: 2015.

the lake and lagoon. Also for the dunes minimal variations over time in zone shape and size are removed by using the most seaward position of all contour lines. Consequently, only the aeolian zone and mixed zones change in shape and size over time. The volumetric change between two consecutive measurements is determined for these zones within the smaller contour:

$$\Delta V^n = \hat{A}_\mathrm{c} \cdot \left(\overline{z_\mathrm{b}}^n - \overline{z_\mathrm{b}}^{n-1}\right) \quad \text{where } \hat{A}_\mathrm{c} = \min\left(A_\mathrm{c}^n \ ; \ A_\mathrm{c}^{n-1}\right) \tag{1}$$

with ΔV^n the volume change, A_c^n the surface area of the zone and $\overline{z_\mathrm{b}}^n$ the average bed level in the zone, all in time interval n. The (cumulative) sum over all time intervals of the volume changes in each zone is used in the analysis. By using the smaller of two contours in a comparison, a part of the larger contour is neglected:

$$A^n_{\mathrm{c,neglected}} = \max\left(A_\mathrm{c}^n \ ; \ A_\mathrm{c}^{n-1}\right) - \hat{A}_\mathrm{c} \tag{2}$$

The neglected area of the zone with the largest change in size, the aeolian zone, is on average 2% and never larger than 8%.

3.3. Spatial variations in porosity

The change in sediment volume is susceptible to changes in porosity. In order to relate the changes in sediment volume to the transport of sediment mass, variations in porosity need to be accounted for. Porosity values in the Sand Motor domain are obtained from core samples and used to account for the spatial variations in porosity. The core samples have a diameter of 8 cm and depth of 10 cm from the bed surface in an attempt to capture the porosity in the aeolian active layer of the bed. Each sample is dried and submerged in water to determine the porosity. For comparison, all presented sediment volumes in this paper are converted to a hypothetical porosity of 40% according to:

$$V_{40\%} = V \cdot \frac{1-p}{1-40\%} \tag{3}$$

where V [m^3] is the measured sediment volume and p [-] the porosity.

4. Results

The overall sediment budget of the Sand Motor domain is determined given morphological change in the net aeolian erosion and net aeolian de-

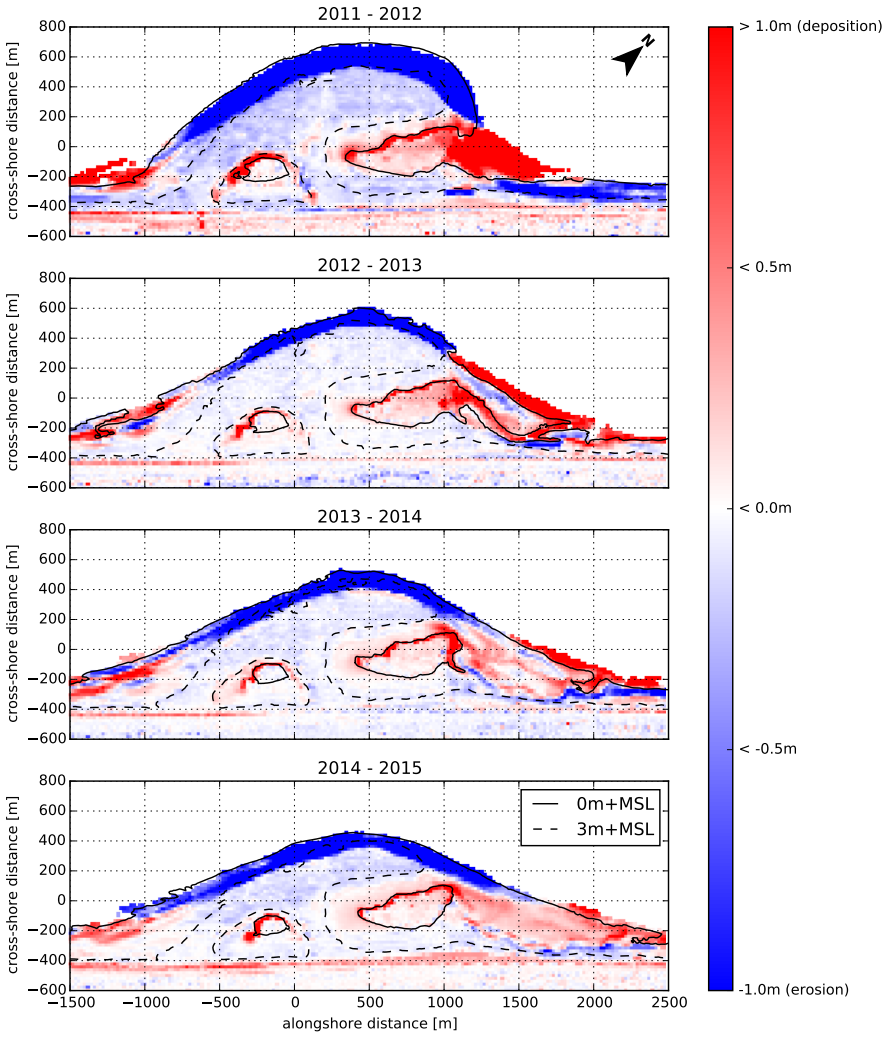

Figure 4: Yearly sedimentation and erosion above 0 m+MSL in the Sand Motor domain. Comparisons are made between the September surveys of each year.

Table 2: Measured porosity values in the Sand Motor domain. Each area is sampled at three different locations. The results per area are presented in ascending order. The last column presents the average porosity for each area that is used to convert the sediment volumes presented in this paper to a hypothetical porosity of 40%.

Area	Porosity			
	min.		max.	avg.
Aeolian zone	39.0%	39.4%	40.2%	39.5%
Mixed zone (north)	38.4%	39.8%	40.8%	39.7%
Mixed zone (south)	37.1%	38.4%	38.4%	38.0%
Dunes	36.1%	36.3%	37.1%	36.5%
Dune lake	34.7%	34.9%	36.3%	35.3%
Lagoon	46.3%	47.3%	49.0%	47.6%

position zones for the period between September 1, 2011 and September 1, 2015 (Figure 4).

4.1. Morphological change and porosity

The net morphological change within the 3 m+MSL contour can be accredited entirely to aeolian sediment transport as this area is not significantly affected by marine processes since the construction of the Sand Motor. Also the net contribution of alongshore sediment fluxes are assumed to be relatively small given that the beach width (< 100 m) is small compared to the alongshore span of the measurement domain (4 km). Within the 3 m+MSL contour sediment is deposited in the dunes and eroded from the aeolian zone.

The morphological change in the dune lake and the closed end of the lagoon is assumed to be driven predominantly by wind. Hydrodynamic forcing and consequently marine deposits in these zones diminished quickly over time, while significant amounts of fine aeolian deposits are found along the southwestern to northwestern shores.

The aeolian contribution to the morphological change in the mixed zones cannot be determined directly due to the presence of both marine and aeolian forces. However, by balancing the changes in sediment volume in the net aeolian deposition zones with the changes in sediment volume in the net aeolian erosion zones the aeolian sediment supply from the mixed zones is estimated.

18 porosity measurements from six zones (Table 2) are used to convert all measured sediment volumes to a hypothetical porosity of 40%.

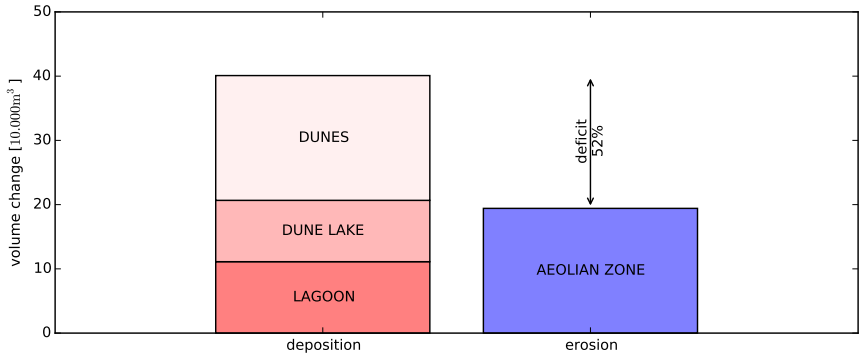

Figure 5: Aeolian sediment budgets in the Sand Motor domain in the period between September 1, 2011 and September 1, 2015.

4.2. Aeolian sediment budgets

The aeolian zone consistently provides less sediment than is deposited in the dunes, dune lake and lagoon (Figure 5). Over the four years since construction of the Sand Motor the volume deficit accumulates to $21 \cdot 10^4$ m^3, which is 52% of the total sediment accumulation of $40 \cdot 10^4$ m^3. The total wind transport capacity (or cumulative theoretical sediment transport volume) in this period is roughly estimated as $110 \cdot 10^4$ m^3 (Appendix A). As the actual sediment transport rates appear to be only about 35% of the wind transport capacity, the Sand Motor can be classified as an availability-limited system.

Late January 2012, the surveys show a net volume deficit of zero, while subsequent surveys show a more or less linear growth of the volume deficit (Figure 6). Fitting a linear trend reveals an average growth rate of $5.2 \cdot 10^4$ m^3/yr, which is 67% of the total sediment accumulation rate of $7.7 \cdot 10^4$ m^3/yr ($R^2 = 0.96$). The increase in growth rate of the volume deficit is likely caused by a significant decrease of the sediment contribution from the aeolian zone. The erosion from the aeolian zone in the first half year after construction of the Sand Motor exceeds the total erosion in the four years thereafter, while sediment continued to be accumulated in the dunes, dune lake and lagoon. The surface area of the aeolian zone decreased continuously (Figure 7).

The diminishing of the aeolian sediment supply from the aeolian zone is also reflected in the average bed level within the 3 m+MSL contour of

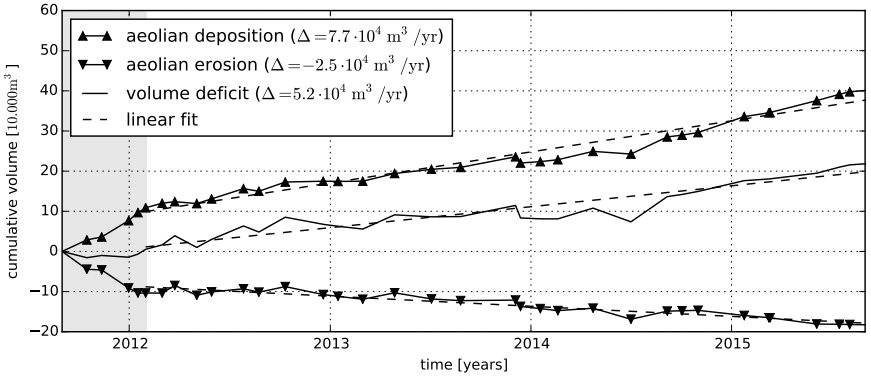

Figure 6: Cumulative change in sediment volume of all net aeolian erosion and net aeolian deposition zones and the volume deficit. For the linear fit the period prior to February 2012 is discarded (shaded).

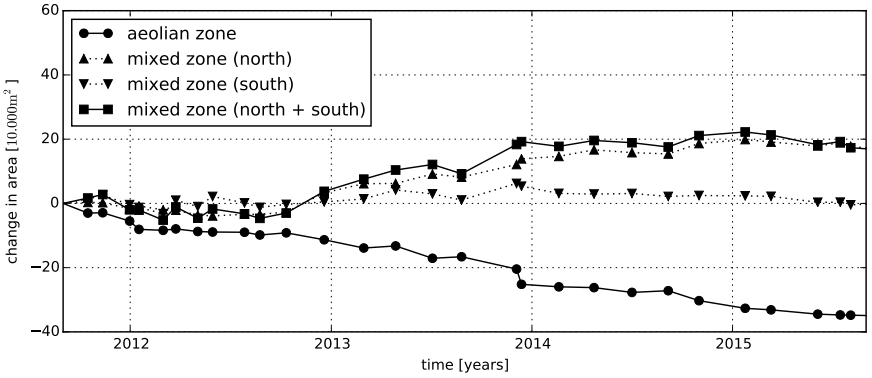

Figure 7: Change in size of aeolian zone and mixed zones since construction of the Sand Motor in 2011.

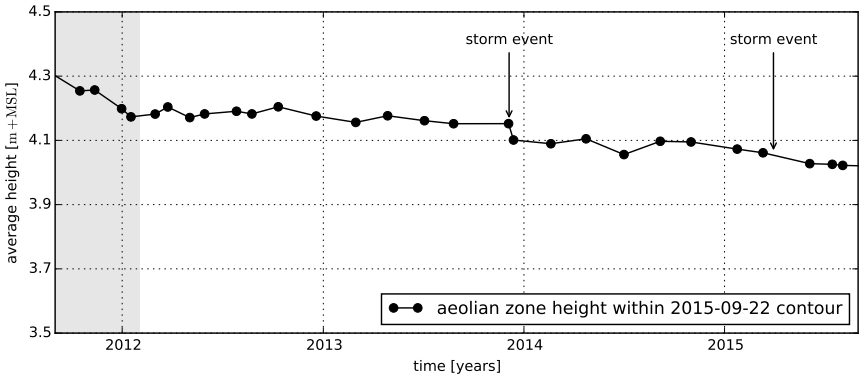

Figure 8: Average height of the aeolian zone in the most recent contour.

September 22, 2015 (Figure 8). The bed level within this contour has been almost constant since the volume deficit started to grow steadily from late January 2012. Only a few periods of significant erosion can be distinguished that can be related to storm events. Most notably, the event of December 5, 2013 with wind speeds up to 34 m/s. That day $1.5 \cdot 10^4$ m^3 of sediment was eroded from within the 3 m+MSL contour of September 22, 2015, which is 52% of the total erosion that year. Although this event is among the few events during which the runup levels exceeded the 3 m+MSL level (Figure 2), the erosion can still be accredited to wind as the 3 m+MSL contour of September 22, 2015 was located about 100 m landward of the 3 m+MSL contour at the time of the storm event. Therefore the bed level in the more recent contour was not affected by the surge, which is confirmed by observations from a local permanent camera station.

In general, the use of the 3 m+MSL contour as divide between the areas with and without marine influence appears to be valid for almost the entire four years after construction of the Sand Motor. Only four events have been registered in which runup levels exceeded the 3 m+MSL level (Figure 2). Observations from a local permanent camera station indicate that only during the event of December 5, 2013 the surface of the aeolian zone was significantly affected by tides and waves. Pre- and post-storm topographic surveys that are available for this event indicate that the marine erosion from the flooded areas above the 3 m+MSL level was less than $1 \cdot 10^4$ m^3.

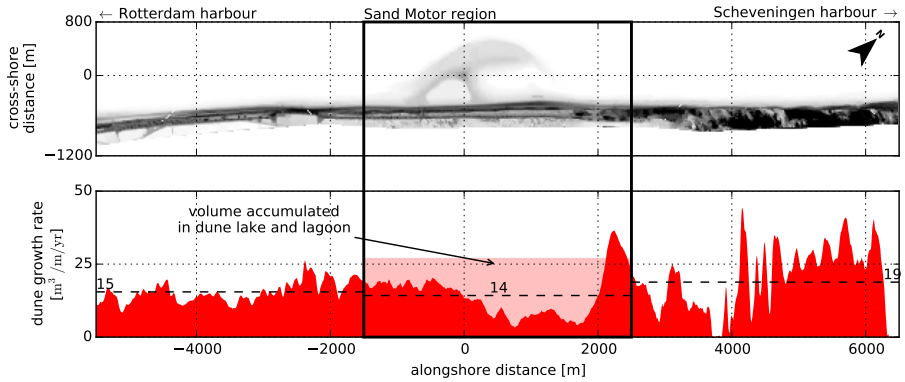

Figure 9: Comparison sediment accumulation rates in dunes (>3 m+MSL) for Sand Motor domain and adjacent coasts. Airborne lidar measurements from January 2012 until January 2015 are used. Horizontal dashed lines indicate local averages. The box indicates the Sand Motor domain depicted in previous figures.

4.3. Alongshore variation

The sediment deposits in the dunes show an alongshore variation. A depression in dune growth is observed in the lee of the dune lake and lagoon (Figure 9). South of the dune lake and in between the dune lake and lagoon a passage for aeolian sediment transport is present, which seems to result in a locally elevated dune growth. The average dune growth of 14 $m^3/m/yr$ in the Sand Motor domain is low compared to the dune growth rate along the adjacent southern (15 $m^3/m/yr$) and northern (19 $m^3/m/yr$) beach stretches. However, aeolian deposits in the dune lake and lagoon are of the same order of magnitude resulting in a total average sediment deposition of 27 $m^3/m/yr$ in the Sand Motor domain, which is on average 56% higher than along the adjacent coasts.

5. Discussion

The volume deficit between the net aeolian erosion and net aeolian deposition zones can be accredited to the mixed zones that are affected by both marine and aeolian processes. The mixed zones in the Sand Motor domain are consequently estimated to provide 67% of the aeolian sediment in the Sand Motor domain. The aeolian sediment supply from the mixed zones is therefore significant, but still small compared to the 98% reported by Jackson

et al. (2010). The importance of the mixed zone cannot be explained by the size of the surface area as the mixed zones are initially smaller than the other main sediment source: the aeolian zone (Figure 7). Only from 2013 onward the surface area of the mixed zones exceed the area of the aeolian zone. However, the increase in surface area of the mixed zones is concentrated in the north where a low-lying spit develops (Figure 4). Given the dominant south to southwesterly wind direction and their position with respect to the lagoon that separates the spit from the dunes, it is unlikely that these intertidal beaches, provide a significant amount of sediment to dunes, dune lake and lagoon. Therefore, despite the periodic flooding and a size that is 40% – 60% smaller than the aeolian zone, the mixed zone (south) appears to provide the majority of the aeolian sediment in the Sand Motor domain.

5.1. Sources of inaccuracies

By accrediting the volume deficit to the mixed zones it is assumed that no sediment is exchanged over the boundaries of the Sand Motor domain and the sediment volume balance is thus closed. This assumption is not strictly valid, but the external sediment exchange with the Sand Motor domain is limited compared to the total sediment accumulation of $40 \cdot 10^4$ m^3.

The predominantly southwesterly wind direction might blow sediment over the lateral borders that is not taken into account. However, the net alongshore sediment supply to the Sand Motor domain is estimated to be two orders smaller than the net onshore sediment supply, or less than 1% of the total sediment accumulation (Figure 10), because:

1. The onshore and alongshore sediment flux *per meter width* are estimated to be of the same order of magnitude (Appendix A), but the lateral beach cross-section ($<$ 100 m) through which the alongshore flux enters the Sand Motor domain at the southern border is an order of magnitude smaller than the alongshore span of the Sand Motor domain (4 km) through which the onshore flux enters the domain. Therefore, the absolute alongshore contribution to the total sediment volume balance is likely an order of magnitude smaller than the onshore contribution.
2. The contribution of the net alongshore sediment flux that enters the Sand Motor domain at the southern border is at least partially compensated by a net alongshore sediment flux of the same order of magnitude that leaves the domain at the northern border. Therefore, the

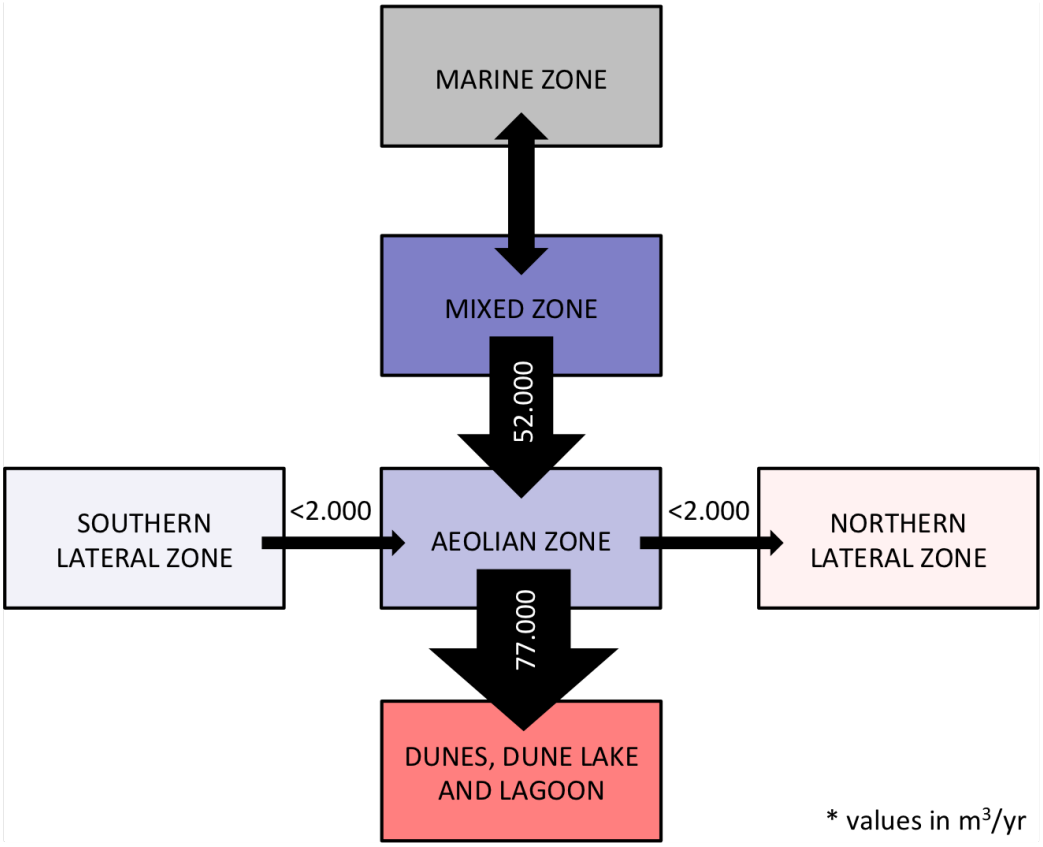

Figure 10: Aeolian sediment budget analysis of the Sand Motor

contribution to the total sediment volume balance of the southern and northern alongshore sediment fluxes combined (alongshore sediment transport gradient) is likely two orders of magnitude smaller than the contribution of the onshore sediment flux.

In reality the contribution of the alongshore sediment fluxes is likely to be even smaller as the sediment fluxes can locally be more onshore directed due to local wind steering. In addition, the estimates of the order of magnitude of the sediment fluxes are likely to be overestimated as possible limitations in sediment availability are ignored.

The influence of marine deposits in the lagoon is estimated to be less than 4% of the total sediment accumulation. 85% of the deposited sediment in the lagoon has the form of a southwesterly infill protruding above water and consisting of loosely packed, fine sediment and is therefore likely from aeolian origin (Figure 4 and Table 2). 15% of the deposited sediment in the lagoon, or 4% of the total sediment accumulation, is spread over a wider area and is possibly from marine origin.

The influence of marine erosion of the aeolian zone during the limited number of storm surges is estimated to be less than $1 \cdot 10^4$ m^3 (Section 4.2), or 2.5% of the total sediment accumulation. Similarly, the influence of the changing size of the aeolian zone is estimated to be 2% of the total erosion in this area (Section 3.2), or less than 1% of the total sediment accumulation.

In summary, the error that is introduced by assuming a closed sediment volume balance is estimated to be less than 9% of the total sediment accumulation. The volume deficit of 67% of the total sediment accumulation that is accredited to aeolian erosion from the mixed zones therefore needs to be nuanced and is estimated to be more than 58%.

5.2. Beach armoring

The relative importance of the mixed zones for aeolian sediment supply can likely be explained by a visually observed beach armor layer that developed in the aeolian zone since construction of the Sand Motor. A beach armor layer can reduce the availability of aeolian sediment significantly (McKenna Neuman et al., 2012). Because the Sand Motor was constructed several meters above common storm surge level, the aeolian zone has never been influenced by waves or tides. Consequently, no process is present that regularly resets the armor layer, except for the occasional high-energy wind

event. Moreover, salt crusts that form due to salt spray have a similar effect on the sediment availability as an armor layer. Small concentrations of salt (≤ 7 mg/g) can already reduce the sediment availability by a factor two (Nickling and Ecclestone, 1981).

In contrast, no beach armor layer or salt crusts develop in the mixed zones as periodic flooding and related wave-reworking regularly deposit marine sediments, mix the top layer of the bed, and wash shells and shell fragments away. In addition, onshore bar migration and welding periodically provide additional unarmored sediment that can be entrained by the wind during low water (Houser, 2009; Anthony, 2013). However, aeolian sediment availability in the mixed zones is also limited due to the relatively high soil moisture contents in these areas. Also soil moisture content is known to increase the shear velocity threshold (Wiggs et al., 2004; Edwards and Namikas, 2009; Namikas et al., 2010) and limit the local aeolian sediment availability. Given that the mixed zones appear to be a more important supplier of aeolian sediment than the aeolian zone, limitations in sediment availability due to beach armoring seems to outweigh limitations due to high moisture contents.

During a storm event even shell fragments and shells can be mobilized. Consequently, the beach armor layer itself might be transported and its reducing effect on the sediment availability is (partially) neutralized. Storm events are regularly accompanied with surges that prevent wind erosion of the mixed zones. Entrainment of sediment therefore starts at a relatively high point along the fetch and much of the sediment transport capacity can be used for erosion of the aeolian zone, which contributes to the removal of the beach armor layer. If the surge is high enough it can also remove the beach armor layer by wave action or bury it by deposition of marine sediments. The removal or burial of the beach armor layer can elevate sediment availability from the aeolian zone also after the the storm passed. Only after development of a new beach armor layer the sediment availability and transport rates approach the pre-storm situation.

5.3. Mega nourishments as coastal protection

The Sand Motor mega nourishment shows a morphological development that is significantly different from natural beaches or the original Delfland coast. Aeolian sediment supply at the Sand Motor shows larger spatial variations compared to natural beaches, while dune growth rates lag behind compared to the adjacent coastal stretches. It can be questioned if such exotic behavior is desired for a coastal protection that aims to stimulate

natural processes, or that, for example, it would be beneficial not to construct future mega nourishments above local storm surge level and prevent compartmentalization of the beach.

In this context, it is interesting to consider what would happen if the Sand Motor was constructed up to local storm surge level (3 m+MSL). The vast aeolian zone would not exist as the entire Sand Motor would be flooded at least once a year. Compartmentalization would be minimized and aeolian sediment availability be maximized as the formation of deflation lag deposits is counteracted by wave-reworking. The dune lake and lagoon would be filled in up to three times faster due to transport-limited aeolian sediment supply. Soon, all aeolian sediment transport pathways would end in the dunes, resulting in an up to six times larger dune growth than currently observed. Marine sediment transport would enhance these relatively rapid changes as more sediment is redistributed within the Sand Motor domain to the lagoon, dune lake and offshore by overwash.

A lower construction height of the Sand Motor would therefore result in a more rapid and more localized redistribution of sediment. Both rapid and localized redistribution are at odds with the purpose of the Sand Motor to nourish the entire Holland coast over a period of two decades. The static behavior of the supratidal areas of Sand Motor might therefore prove to be a crucial design criterion of a mega nourishment.

6. Conclusions

A sediment budget analysis is used to identify spatial variations in aeolian sediment deposition and supply, and dune growth in the Sand Motor domain. From the analysis the following conclusions can be drawn regarding aeolian sediment transport and supply in the Sand Motor domain:

1. The (southern) low-lying beaches that are affected by both aeolian and marine processes (mixed zone) currently supply more than 58% of all aeolian sediment deposits in the Sand Motor domain, despite that this area is periodically flooded and 40% – 60% smaller than the upper dry beach areas (aeolian zone) that are only affected by aeolian processes and supply less than 42% of the aeolian deposits;
2. The aeolian sediment supply from the aeolian zone diminished in the first half year after construction of the Sand Motor, likely due to the development of a beach armor layer;

3. The aeolian sediment supply from the aeolian zone tends to increase temporarily during and after a storm event, likely due to (partial) removal of the beach armor layer;
4. The dune growth in the Sand Motor domain is low compared to the adjacent coasts, likely due to blocking of aeolian sediment transport pathways by the dune lake and lagoon.

From the analysis the following conclusions can be drawn regarding mega nourishments in general:

1. The construction height should be a design criterion of any mega nourishment as it governs compartmentalization of the beach due to beach armoring;
2. Compartmentalization of the beach can influence the lifetime and region of influence of a mega nourishment as it affects the balance between local aeolian deposition and regional marine spreading of sediment.
3. The consequences of compartmentalization is not yet fully understood as the contribution of the upper dry beach (aeolian zone) to local aeolian sediment supply can range from 42% as observed at the Sand Motor to less than 2% as reported by Jackson et al. (2010).

Acknowledgements

The work discussed in this paper is supported by the ERC-Advanced Grant 291206 – Nearshore Monitoring and Modeling (NEMO).

A. Theoretical Sediment Transport Volumes

The cumulative theoretical sediment transport volume Q [m^3] in the Sand Motor domain between September 1, 2011 and September 1, 2015 is estimated from hourly averaged measured wind speed u_{10} [m/s] and direction θ_u [°] measured at 10 m height by the KNMI meteorological station in Hoek van Holland (Figure 2). The wind time series are used in conjunction with the formulation of Bagnold (1937) to obtain the instantaneous theoretical sediment transport rate q [kg/m/s] following:

$$q = C\frac{\rho_\mathrm{a}}{g}\sqrt{\frac{d_\mathrm{n}}{D_\mathrm{n}}}\left(u_* - u_{*\mathrm{th}}\right)^3 \tag{A.1}$$

with the shear velocity $u_* = \alpha \cdot u_{10}$ m/s, the shear velocity threshold $u_{*\mathrm{th}} = \alpha \cdot 3.87$ m/s, the conversion factor from free-flow wind velocity to shear velocity $\alpha = 0.058$, the air density $\rho_\mathrm{a} = 1.25$ kg/m^3, the particle density $\rho_\mathrm{p} = 2650.0$ kg/m^3, the gravitational constant $g = 9.81$ m/s^2, the nominal grain size $d_\mathrm{n} = 335$ μm and a reference grain size $D_\mathrm{n} = 250$ μm.

The cumulative theoretical sediment transport volumes in onshore (Q_os [m^3]) and alongshore (Q_as [m^3]) direction are computed by time integration and conversion from mass to volume following:

$$\begin{array}{rcl} Q_\mathrm{os} & = & \sum q \cdot \frac{\Delta t \cdot \Delta y}{(1-p)\cdot\rho_\mathrm{p}} \cdot f_{\theta_u,\mathrm{os}} \quad = \quad 110 \cdot 10^4 \text{ m}^3 \\ Q_\mathrm{as} & = & \sum q \cdot \frac{\Delta t \cdot \Delta x}{(1-p)\cdot\rho_\mathrm{p}} \cdot f_{\theta_u,\mathrm{as}} \quad = \quad 3 \cdot 10^4 \text{ m}^3 \end{array} \tag{A.2}$$

where the temporal resolution $\Delta t = 1$ h, the alongshore span of the measurement domain $\Delta y = 4$ km, the approximate lateral beach width $\Delta x = 100$ m, the porosity $p = 0.4$ and $f_{\theta_u,\mathrm{os}}$ and $f_{\theta_u,\mathrm{as}}$ are factors to account for respectively the onshore and alongshore wind directions only, defined as:

$$\begin{array}{rcl} f_{\theta_u,\mathrm{os}} & = & \max\left(0 \quad ; \quad \cos\left(312\,^\circ - \theta_u\right)\right) \\ f_{\theta_u,\mathrm{as}} & = & \sin\left(312\,^\circ - \theta_u\right) \end{array} \tag{A.3}$$

where θ_u [$^\circ$] is the hourly averaged wind direction and 312 $^\circ$ accounts for orientation of the original coastline.

Note that the difference between the onshore and alongshore cumulative theoretical sediment transport volumes (Equation A.2) of a factor 40 is determined solely by the difference between the onshore and alongshore cross-sections of 4 km and 100 m respectively. The sediment transport volumes per meter width in onshore and alongshore direction are of the same order of magnitude (275 m^3/m and 267 m^3/m respectively).

References

Aagaard, T., Davidson-Arnott, R., Greenwood, B., and Nielsen, J. (2004). Sediment supply from shoreface to dunes: linking sediment transport measurements and long-term morphological evolution. *Geomorphology*, 60(1):205–224. doi:10.1016/j.geomorph.2003.08.002.

Anthony, E. J. (2013). Storms, shoreface morphodynamics, sand supply, and the accretion and erosion of coastal dune barriers in the southern north sea. *Geomorphology*, 199:8–21. doi:10.1016/j.geomorph.2012.06.007.

Bagnold, R. (1937). The transport of sand by wind. *Geographical journal*, pages 409–438.

Borsje, B. W., van Wesenbeeck, B. K., Dekker, F., Paalvast, P., Bouma, T. J., van Katwijk, M. M., and de Vries, M. B. (2011). How ecological engineering can serve in coastal protection. *Ecological Engineering*, 37(2):113–122. doi:10.1016/j.ecoleng.2010.11.027.

Davidson-Arnott, R. G. and Law, M. N. (1990). *Seasonal patterns and controls on sediment supply to coastal foredunes, Long Point, Lake Erie*, pages 177–200. Wiley Chichester.

De Schipper, M., De Vries, S., Ranasinghe, R., Reniers, A., and Stive, M. (2013). Alongshore topographic variability at a nourished beach. In *Coastal Dynamics 2013: 7th International Conference on Coastal Dynamics, Arcachon, France, 24-28 June 2013*. Bordeaux University.

de Schipper, M. A., de Vries, S., Ruessink, G., de Zeeuw, R. C., Rutten, J., van Gelder-Maas, C., and Stive, M. J. (2016). Initial spreading of a mega feeder nourishment: Observations of the sand engine pilot project. *Coastal Engineering*, 111:23–38. doi:10.1016/j.coastaleng.2015.10.011.

de Vriend, H. J., van Koningsveld, M., Aarninkhof, S. G., de Vries, M. B., and Baptist, M. J. (2015). Sustainable hydraulic engineering through building with nature. *Journal of Hydro-environment Research*, 9(2):159–171. doi:10.1016/j.jher.2014.06.004.

de Vries, S., Arens, S. M., de Schipper, M. A., and Ranasinghe, R. (2014). Aeolian sediment transport on a beach with a varying sediment supply. *Aeolian Research*, 15:235–244. doi:10.1016/j.aeolia.2014.08.001.

de Vries, S., Radermacher, M., de Schipper, M., and Stive, M. (2015). Tidal dynamics in the Sand Motor lagoon. In *E-proceedings of the 36th IAHR World Congress*.

Delgado-Fernandez, I., Davidson-Arnott, R., Bauer, B. O., Walker, I. J., Ollerhead, J., and Rhew, H. (2012). Assessing aeolian beach-surface dynamics using a remote sensing approach. *Earth Surface Processes and Landforms*, 37(15):1651–1660. doi:10.1002/esp.3301.

Donchyts, G., Baart, F., Winsemius, H., Gorelick, N., Kwadijk, J., and van de Giesen, N. (2016). Earth's surface water change over the past 30 years. *Nature Climate Change*, 6(9):810–813. doi:10.1038/nclimate3111.

Edwards, B. L. and Namikas, S. L. (2009). Small-scale variability in surface moisture on a fine-grained beach: implications for modeling aeolian transport. *Earth Surface Processes and Landforms*, 34:1333–1338. doi:10.1002/esp.1817.

Grunnet, N. M. and Ruessink, B. (2005). Morphodynamic response of nearshore bars to a shoreface nourishment. *Coastal Engineering*, 52(2):119–137. doi:10.1016/j.coastaleng.2004.09.006.

Hamm, L., Capobianco, M., Dette, H., Lechuga, A., Spanhoff, R., and Stive, M. (2002). A summary of european experience with shore nourishment. *Coastal engineering*, 47(2):237–264. doi:10.1016/S0378-3839(02)00127-8.

Houser, C. (2009). Synchronization of transport and supply in beach-dune interaction. *Progress in Physical Geography*, 33(6):733–746. doi:10.1177/0309133309350120.

Jackson, N. L. and Nordstrom, K. F. (2011). Aeolian sediment transport and landforms in managed coastal systems: a review. *Aeolian research*, 3(2):181–196. doi:10.1016/j.aeolia.2011.03.011.

Jackson, N. L., Nordstrom, K. F., Saini, S., and Smith, D. R. (2010). Effects of nourishment on the form and function of an estuarine beach. *Ecological Engineering*, 36(12):1709–1718. doi:10.1016/j.ecoleng.2010.07.016.

Kocurek, G. and Lancaster, N. (1999). Aeolian system sediment state: theory and mojave desert kelso dune field example. *Sedimentology*, 46(3):505–515. doi:10.1046/j.1365-3091.1999.00227.x.

Lynch, K., Jackson, D. W., and Cooper, J. A. G. (2016). The fetch effect on aeolian sediment transport on a sandy beach: a case study from magilligan strand, northern ireland. *Earth Surface Processes and Landforms*. doi:10.1002/esp.3930.

McKenna Neuman, C., Li, B., and Nash, D. (2012). Micro-topographic analysis of shell pavements formed by aeolian transport in

566 a wind tunnel simulation. *Journal of Geophysical Research*, 117(F4).
567 doi:10.1029/2012JF002381. F04003.

568 Namikas, S. L., Edwards, B. L., Bitton, M. C. A., Booth, J. L., and
569 Zhu, Y. (2010). Temporal and spatial variabilities in the surface mois-
570 ture content of a fine-grained beach. *Geomorphology*, 114:303–310.
571 doi:10.1016/j.geomorph.2009.07.011.

572 Nickling, W. G. and Ecclestone, M. (1981). The effects of soluble salts on
573 the threshold shear velocity of fine sand. *Sedimentology*, 28:505–510.

574 Ojeda, E., Ruessink, B., and Guillen, J. (2008). Morphodynamic response
575 of a two-barred beach to a shoreface nourishment. *Coastal Engineering*,
576 55(12):1185–1196. doi:10.1016/j.coastaleng.2008.05.006.

577 Sherman, D. J., Jackson, D. W., Namikas, S. L., and Wang, J. (1998).
578 Wind-blown sand on beaches: an evaluation of models. *Geomorphology*,
579 22(2):113–133. doi:10.1016/S0169-555X(97)00062-7.

580 Sherman, D. J. and Li, B. (2012). Predicting aeolian sand trans-
581 port rates: a reevaluation of models. *Aeolian Research*, 3(4):371–378.
582 doi:10.1016/j.aeolia.2011.06.002.

583 Stive, M. J. F., de Schipper, M. A., Luijendijk, A. P., Aarninkhof, S. G. J.,
584 van Gelder-Maas, C., van Thiel de Vries, J. S. M., de Vries, S., Henriquez,
585 M., Marx, S., and Ranasinghe, R. (2013). A new alternative to saving our
586 beaches from sea-level rise: the Sand Engine. *Journal of Coastal Research*,
587 29(5):1001–1008. doi:10.2112/JCOASTRES-D-13-00070.1.

588 Stockdon, H. F., Holman, R. A., Howd, P. A., and Sallenger, A. H. (2006).
589 Empirical parameterization of setup, swash, and runup. *Coastal engineer-*
590 *ing*, 53(7):573–588. doi:10.1016/j.coastaleng.2005.12.005.

591 van der Wal, D. (1998). The impact of the grain-size distribution of nourish-
592 ment sand on aeolian sand transport. *Journal of Coastal Research*, pages
593 620–631.

594 van der Wal, D. (2000). Grain-size-selective aeolian sand transport on a
595 nourished beach. *Journal of Coastal Research*, pages 896–908.

Van Slobbe, E., De Vriend, H., Aarninkhof, S., Lulofs, K., De Vries, M., and Dircke, P. (2013). Building with nature: in search of resilient storm surge protection strategies. *Natural hazards*, 65(1):947–966. doi:10.1007/s11069-012-0342-y.

Waterman, R. E. (2010). *Integrated coastal policy via Building with Nature*. TU Delft, Delft University of Technology.

Wiggs, G. F. S., Baird, A. J., and Atherton, R. J. (2004). The dynamic effects of moisture on the entrainment and transport of sand by wind. *Geomorphology*, 59:13–30. doi:10.1016/j.geomorph.2003.09.002.